

RESEARCH ARTICLE

Ecosystem Evapotranspiration as a Response to Climate and Vegetation Coverage Changes in Northwest Yunnan, China

Hao Yang^{1,2,4}, Peng Luo^{1,3*}, Jun Wang^{1,2,4}, Chengxiang Mou^{1,4}, Li Mo^{1,4}, Zhiyuan Wang⁵, Yao Fu⁶, Honghui Lin², Yongping Yang⁶, Laxmi Dutt Bhatta⁷

1 Key Laboratory of Mountain Ecological Restoration and Bioresource Utilization of Chinese Academy of Sciences, Chengdu Institute of Biology, Chinese Academy of Sciences, Chengdu, China, **2** College of Life Sciences, Sichuan University, Chengdu, China, **3** Ecological Restoration and Biodiversity Conservation Key Laboratory of Sichuan Province, Chengdu Institute of Biology, Chinese Academy of Sciences, Chengdu, China, **4** University of Chinese Academy of Sciences, Beijing, China, **5** Yunnan Academy of Agricultural Sciences, Kunming, China, **6** Kunming Institute of Botany, Chinese Academy of Sciences, Kunming, China, **7** International Centre for Integrated Mountain Development, Kathmandu, Nepal

* luopeng@cib.ac.cn



OPEN ACCESS

Citation: Yang H, Luo P, Wang J, Mou C, Mo L, Wang Z, et al. (2015) Ecosystem Evapotranspiration as a Response to Climate and Vegetation Coverage Changes in Northwest Yunnan, China. PLoS ONE 10 (8): e0134795. doi:10.1371/journal.pone.0134795

Editor: Shilong Piao, Peking University, CHINA

Received: April 10, 2015

Accepted: July 14, 2015

Published: August 3, 2015

Copyright: © 2015 Yang et al. This is an open access article distributed under the terms of the [Creative Commons Attribution License](http://creativecommons.org/licenses/by/4.0/), which permits unrestricted use, distribution, and reproduction in any medium, provided the original author and source are credited.

Data Availability Statement: The primary dataset of the manuscript contains two parts: remote sensing image data and meteorological data. Remote sensing image data are available from Goddard Space Flight Center, NASA (http://adsweb.nascom.nasa.gov/browse_images) for free downloading. Meteorological data are available from Climatic Data Center, National Meteorological Information Center, China Meteorological Administration (<http://cdc.nmic.cn/home.do>). According to licensing agreement of China Metrological Data Sharing Service System, all interested researchers can register and sign the licensing agreement for data availability.

Abstract

Climate and human-driven changes play an important role in regional droughts. Northwest Yunnan Province is a key region for biodiversity conservation in China, and it has experienced severe droughts since the beginning of this century; however, the extent of the contributions from climate and human-driven changes remains unclear. We calculated the ecosystem evapotranspiration (ET) and water yield (WY) of northwest Yunnan Province, China from 2001 to 2013 using meteorological and remote sensing observation data and a Surface Energy Balance System (SEBS) model. Multivariate regression analyses were used to differentiate the contribution of climate and vegetation coverage to ET. The results showed that the annual average vegetation coverage significantly increased over time with a mean of 0.69 in spite of the precipitation fluctuation. Afforestation/reforestation and other management efforts attributed to vegetation coverage increase in NW Yunnan. Both ET and WY considerably fluctuated with the climate factors, which ranged from 623.29 mm to 893.8 mm and −51.88 mm to 384.40 mm over the time period. Spatially, ET in the southeast of NW Yunnan (mainly in Lijiang) increased significantly, which was in line with the spatial trend of vegetation coverage. Multivariate linear regression analysis indicated that climatic factors accounted for 85.18% of the ET variation, while vegetation coverage explained 14.82%. On the other hand, precipitation accounted for 67.5% of the WY. We conclude that the continuous droughts in northwest Yunnan were primarily climatically driven; however, man-made land cover and vegetation changes also increased the vulnerability of local populations to drought. Because of the high proportion of the water yield consumed for subsistence and poor infrastructure for water management, local populations have been highly vulnerable to climate drought conditions. We suggest that conservation of native vegetation and development of water-conserving agricultural practices should be implemented as adaptive strategies to mitigate climate change.

Funding: This research was funded by the National Natural Science Foundation of China (31170432), the Basic Study Project of Science & Technology Ministry (2012FY110300), the International Center for Integrated Mountain Development (HICAP), the CEPF Project of Shan Shui Conservation Center (201204003), and the John D. and Catherine T. MacArthur foundation (104115). The funders had no role in study design, data collection and analysis, decision to publish, or preparation of the manuscript.

Competing Interests: The authors have declared that no competing interests exist.

Introduction

Climate change had influences on biodiversity and socio-economic systems primarily through increasing temperatures and climate-related disasters [1, 2]. Improving the capacity of the environment to adapt to continuous climate change is vital for the sustainable development of human society and economic systems [3, 4]. Therefore, it is imperative to understand vulnerability of systems and employ corresponding adaptive strategies for biodiversity conservation and adaptive management. Yunnan Province, which is located in Southwest China, is a key area for biodiversity because its vast mountains host more than 18,000 high plant species and 1,836 vertebrate species, which account for 51.6% of the total plants and 54.8% of the total vertebrate species in China [5], respectively. Since the last decade, this area has experienced continuous and intensifying drought conditions, especially in spring, which have led to great social and economic losses [6–8]. These continuous droughts are of significant concern globally and nationally because they are a typical example of the influence of climate change on the sustainability of ecological and social systems in a biodiversity hotspot. Understanding the reasons for increased drought conditions is important for developing adaptive strategies for both conservation and development.

In general, drought can be attributed to climate and anthropogenic activities. Global aridity, especially in Africa, Southern Europe, East and South Asia, and Eastern Australia since the late 1970s has been attributed to natural variations in the El Niño-Southern Oscillation (ENSO), tropical Atlantic sea surface temperatures, Asian monsoons, and global warming [9]. Human activities have also triggered or aggravated drought by changing aerosols concentrations [10], altering land use/land cover [11–14], and increasing water demand along with social development [15]. A tendency of climate warming over the past 50 years was observed in Yunnan [16, 17], and the moisture or precipitation deficiency in combination with increasing temperatures accounted for drought conditions [18]. However, a number of studies have found that deficiencies during droughts were within the range of variations observed during historical climatic drought events [19, 20]. Therefore, the continuous droughts occurring in Yunnan could not be fully explained by climate reasons alone. Although the potential effects of human activities on droughts have been widely discussed [21–23], empirical studies have not been conducted to determine the extent of climate-change or human-activity contributions to the drought.

Drought causes shortages of available water for the ecological and social systems [24] and occurs when the ability of the ecosystem to provision water is lowered, which aggravates drought damage. The water provision function of an ecosystem can be measured by its water yield (WY), which is the sum of runoff and soil undercurrent after plant transpiration, surface evaporation, and vegetation/soil retention [25]. In addition to precipitation, evapotranspiration (ET) is the largest factor influencing WY in water balance equations, which is greatly altered by vegetation dynamics and characteristics [26]. Higher ET results in less water provision to the social system, making it more vulnerable to climatic drought. In recent decades, Yunnan underwent rapid economic development and the most dramatic land-use and land-cover changes in its history [14, 27–29]. The natural vegetation of the area has been significantly modified by increased human utilization, and most of its barren hilly lands have been re-vegetated in massive afforestation and reforestation efforts [14, 30–32]. Therefore, determining the relationship between the dynamics of ET and vegetation changes is crucial to understanding the causes of droughts and determining the increasing vulnerability of the social system to climatic drought in this hotspot area.

We hypothesized that the vegetation coverage changes induced by afforestation/reforestation and other vegetation management activities over the past 13 years have increased the water consumption (ET) and lowered the ecosystem's water provision capability, which may

eventually reduce the social system's resilience to manage water shortage caused by climatic drought. Northwest (NW) Yunnan is an internationally recognized key area of biodiversity conservation in China [33], and it was selected as the study area to test this hypothesis. We utilized a surface energy balance system (SEBS) model to calculate the regional ET according to relevant meteorological data and remote sensing data from 2001 to 2013. We also analyzed the correlations among ET, climate, and vegetation coverage to 1) measure the ecohydrological effects of climate and vegetation coverage changes and 2) analyze and discuss the impact of climate and vegetation coverage changes on droughts in NW Yunnan. The results of this study may be used as a guide in the planning of adaptive strategies for sustainable development in this globally important area of biodiversity conservation.

Study Area

As a part of the Hengduan Mountains, one of the 17 critical regions for biodiversity conservation and the world's most diverse temperate mountain forests [34, 35], NW Yunnan has experienced significant vegetation changes because of rapid economic development and massive afforestation/reforestation programs (i.e., National Forest Protection Plan) [14, 30, 36]. NW Yunnan is located in the east of the Himalayas (24°38' N–29°15' N, 98°05' E–101°16' E) at elevations varying from 648 m to 6,740 m. This area is in the upstream area of four major rivers (Yangtze, Mekong, Salween, and Irrawaddy) in Asia and possesses unique ecological functions [37], especially as the water source area to over 100 million people downstream. Diverse and complicated topography in this area create a variety of microclimates [38]. In general, monsoons bring moisture in summer, with most of the precipitation falling between June and September. The mean annual temperature in this area is 12.3°C and the mean annual rainfall is 1,013 mm.

The land area of NW Yunnan accounts for only 0.4% of the total area in China; however, it hosts 20% of the high plant species and approximately one quarter to one-third of the total animals in China [39]. Evergreen broadleaf forest and mixed forest are the major forest types, alpine grassland is also common [37]. Traditional mountain agriculture is still the major livelihood for its rural population. NW Yunnan covers four administrative prefectures: Nujiang, Diqing, Dali, and Lijiang (Fig 1). Dali and Lijiang are relatively more densely populated and developed, with population densities of 118.6 and 59.5 people per km², respectively. Compared with Dali and Lijiang, Nujiang and Diqing are less populated, with densities of 36.6 and 17.0 people per km², respectively [40]. Continuous droughts over the last decade in NW Yunnan, especially in Dali and Lijiang, have reduced agricultural production and triggered severe domestic water shortages (Climate Communique of Dali Prefecture: http://dl.xxgk.yn.gov.cn/z_m_003/Info_More.aspx?Classid=126584).

Data Source

Moderate Resolution Imaging Spectroradiometer (MODIS) L1B time-series data (MOD021KM, MOD03) from 2001 to 2013 were selected for the estimates of ET and WY because Terra MODIS began to send data in April 2000. All of the MODIS products were downloaded freely from the NASA website (http://ladsweb.nascom.nasa.gov/browse_images). We obtained one to three images every month for the requirement of cloud-free images or quasi-cloud-free images, which met our needs. For fraction of vegetation coverage estimation, MODIS level 3 monthly vegetation indices (MOD13A3) were download from the same website. Digital elevation model (DEM) data were obtained from the Shuttle Radar Topographic Mission (SRTM) project (<http://srtm.csi.cgiar.org/SELECTION/listImages.asp>) with 90 m

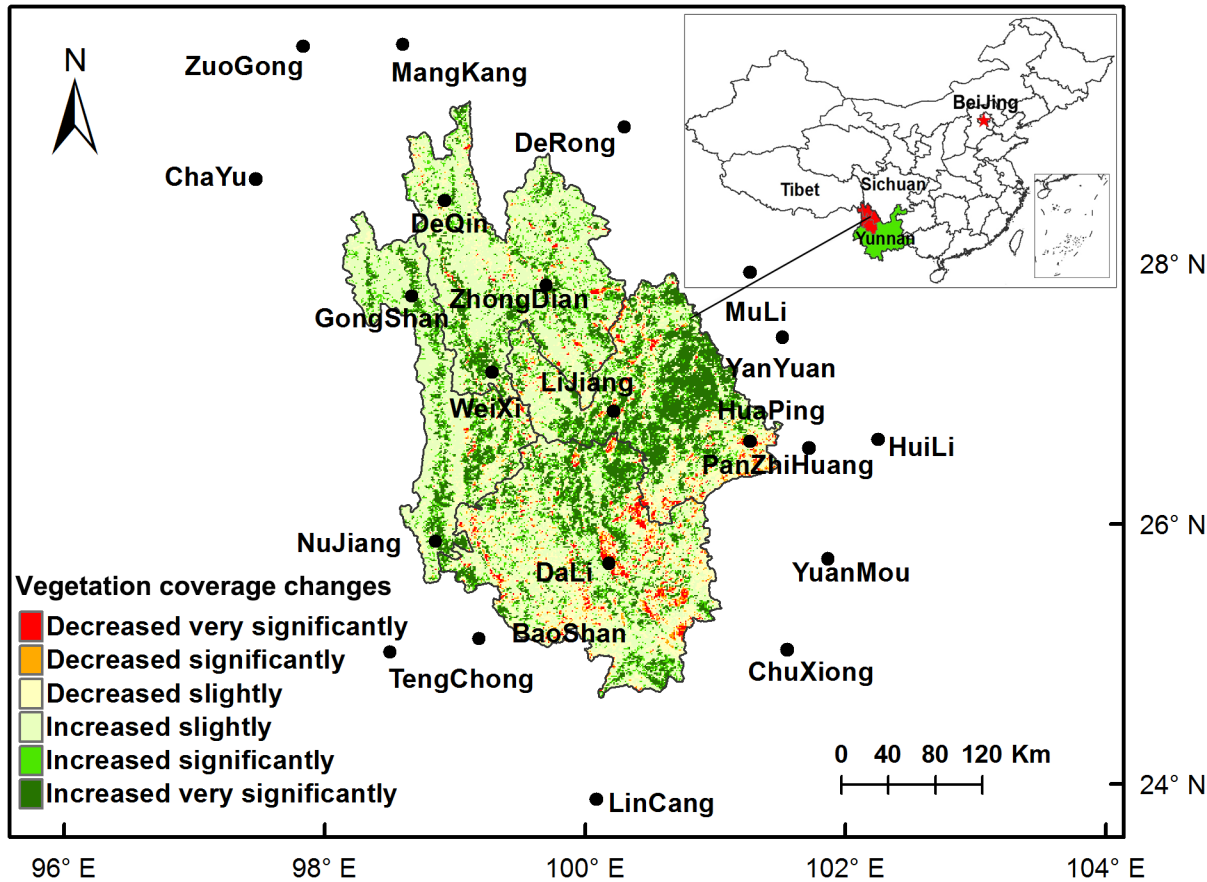


Fig 1. Locations of the 21 meteorological stations and vegetation coverage changes over past 13 years. The trend of vegetation coverage changes from 2001 to 2013 is estimated by linear trend analysis. F-test is employed to test significance of the trends. The increase or decrease trends of vegetation coverage are categorized into three levels: very significantly ($P < 0.01$), significantly ($P < 0.05$), and slightly ($P > 0.05$).

doi:10.1371/journal.pone.0134795.g001

spatial resolution, which were prepared to calculate the ET of the heterogeneous underlying surface (NW Yunnan) in SEBS.

Meteorological data were downloaded from the China Meteorological Data Sharing Service System (<http://cdc.nmic.cn/home.do>), and data from 21 weather stations in the vicinity of the research area were obtained for 2001 and 2013 (Fig 1).

Methods

ET and WY calculation

WY can be calculated as the difference between precipitation and ET [41–43]. The widely used remote sensing model SEBS was chosen to calculate the ET of heterogeneous land surfaces according to satellite data and meteorological information at proper scales [44, 45]. The model is based on traditional energy-balance equations, and it successfully used in different studies worldwide [46–49]. Su et al. proposed the SEBS model [50]. The surface energy balance is commonly written as follows:

$$\lambda E = R_n - G_0 - H \quad (1)$$

where λE is the turbulent latent heat flux (λ is the latent heat of vaporization and E is the actual

ET), R_n is the net radiation, G_0 is the soil heat flux, and H is the sensible heat flux. Calculation methods of above variables were detailed by Su et al. [50].

Comparing with other energy residual methods, the SEBS model improved the following two aspects. First, based on κB^{-1} models of full canopy and bare soil surface, it produced reliable estimates of κB^{-1} that were partly covered with vegetation, which was used for the scalar roughness height of heat transfer and H estimation. Second, every pixel was placed under the dry and wet limits to avoid uncertainty of spatial interpolation of meteorological data. SEBS assumed that the latent heat flux (λE) was zero at the dry limit because of the limitation of soil moisture, but it took place at potential rate in the wet limit. As a result, sensible heat flux reached its maximum and minimum values, respectively, which can be expressed as:

$$H_{dry} = R_n - G_0 \tag{2}$$

$$H_{wet} = R_n - G_0 - \lambda E_{wet} \tag{3}$$

According to Eqs 1, 2 and 3, the relative evaporative fraction (EF_r) and evaporative fraction (EF) then can be calculated as:

$$EF_r = \frac{\lambda E}{\lambda E_{wet}} = 1 - \frac{H - H_{wet}}{H_{dry} - H_{wet}} \tag{4}$$

$$EF = \frac{\lambda E}{R_n - G_0} = \frac{EF_r \lambda E_{wet}}{R_n - G_0} \tag{5}$$

By inverting Eq 5, the actual latent heat flux can be obtained, then daily ET can be calculated as:

$$ET_{daily} = 8.64 \times 10^7 \times EF_{daily} \times \frac{R_n - G_0}{\lambda \rho_w} \tag{6}$$

where ET_{daily} is the actual daily evapotranspiration (mm/d), ρ_w is the water density. Here, R_n represents daily mean net radiation, and G_0 is daily mean soil heat flux which is close to zero. EF_{daily} is the daily mean evaporation fraction. EF_{daily} can be replaced by EF as the model assumes that EF remained relatively stable during one day.

We multiplied the reference ET fraction by ET_0 and completed the extension at the appropriate time scale. The Food and Agriculture Organization (FAO) of the United Nations' report FAO-56 defined ET_0 as the ET rate from a reference surface that does not experience water shortages [51], and it is calculated as follows:

$$ET_0 = \frac{0.408\Delta(R_n - G_0) + \gamma \frac{900}{T+273} v_2 (e_s - e_a)}{\Delta + \gamma(1 + 0.34v_2)} \tag{7}$$

This extension method originated with the model mapping ET with internalized calibration (METRIC) [52], which is similar to the K_C - ET_0 approach [51]. Considering the minimal variation in reference ET fraction over several weeks, we can use the following equation to determine the total monthly or seasonal ET:

$$ET_{period} = \sum_{i=m}^n [(ET_r F_i)(ET_{0i})] \tag{8}$$

where ET_{period} is the cumulative ET, $ET_r F$ is the reference ET fraction resulting from ET

calculated by SEBS over the reference ET (ET_r), $ET_r F_i$ is the interpolated $ET_r F$ for day i and ET_{0i} is the daily ET_0 for day i .

The precipitation value was obtained from the meteorological station in this area and interpolated to polygon data at the regional scale with the inverse distance weighted method. WY was calculated by determining the precipitation and subtracting the ET.

Estimate precision of the SEBS model

Because of the lack of availability of ET field data, free water surface evaporation data measured by evaporators at meteorological stations were used to validate the precision of the estimated ET. A 20 m² evaporation tank was recommended by the World Meteorological Organization as the standard evaporimeter to measure free water surface evaporation [53]. In China modified GGI-3000, named E601 evaporator (area 0.3 m²), is a common tool used to observe evaporation in meteorological stations [54]. We used the water surface evaporation of Erhai Lake obtained from the adjacent Dali meteorological station in NW Yunnan to estimate the precision of the SEBS model. The converted coefficient between the 20 m² evaporation tank and E601 was 0.97 in Dali [55]. The root mean square deviation (RMSD) and mean absolute percent error (MAPE) were used to compare the differences between the estimated ET and measured value that was converted to the ET of the 20 m² evaporation tank according to the coefficient. These two variables were calculated as follows:

$$RMSD = \left| \frac{1}{n} \sum_{i=1}^n (P_i - O_i)^2 \right|^{1/2} \tag{9}$$

$$MAPE = \frac{100}{n} \sum_{i=1}^n \frac{|P_i - O_i|}{O_i} \tag{10}$$

where n is the number of samples, P_i is the evaporation estimated by the SEBS model, and O_i is the observed value by the E601 evaporator.

Image processing

All of the obtained images were reprojected and converted to geographic longitude/latitude WGS-1984 projections in geo-tiff format using the MODIS Swath tool. MOD021KM and MOD03 products were used to calculate the surface physical parameters, such as albedo, vegetation coverage, emissivity, surface temperature, and instantaneous normalized difference vegetation index (NDVI), via ILWIS 3.8.3 and ArcGIS 10.

Monthly NDVI data were used to estimate the vegetation coverage based on the dimidiate pixel model. In the dimidiate pixel model, a pixel consists of vegetation and non-vegetation. Thus, the ratio of vegetation coverage to the pixel (vegetation fraction) represents the vegetation coverage, and this model is widely used to estimate vegetation coverage [56, 57]. This variable was calculated as follows [58, 59]:

$$F_c = (NDVI - NDVI_{soil}) / (NDVI_{veg} - NDVI_{soil}) \tag{11}$$

where $NDVI_{soil}$ is the NDVI value of bare soil or non-vegetation coverage, and $NDVI_{veg}$ represents the NDVI value of full vegetation coverage at a pixel. Given 5% vote of confidence, $NDVI_{veg}$ and $NDVI_{soil}$ were set as the maximal and minimal NDVI, respectively [59].

All of the meteorological data were interpolated into gridded data at a spatial resolution of 0.01 degree cell size with the inverse distance weighted method. These data were used in the

SEBS model to calculate the relative evaporation and daily ET as well as in the calculations for the reference ET (ET_0) in the ET_0 calculator.

Statistical analysis

Linear trend estimation was employed to quantify the ET and WY trends in every pixel as follows:

$$K = \frac{n \times \sum_{i=1}^n i \times S_i - (\sum_{i=1}^n i)(\sum_{i=1}^n S_i)}{n \times \sum_{i=1}^n i^2 - (\sum_{i=1}^n i)^2} \tag{12}$$

where S_i is the cumulative ET or WY and i is the sequence number of years (i.e., 1 to n). $K > 0$ and $K < 0$ indicate that the ET or WY of this pixel increases or decreases over time, respectively.

A multivariate linear regression analysis was used to measure the contribution of climatic factors and vegetation changes to ET, and vegetation coverage was considered the fixed variable of the stepwise regression equation. Moreover, the main climatic factors were filtered by the stepwise backwards selection method based on the analysis principle of significance, which could eliminate climate variables with minimal predictive effect. Then, the absolute value of the standardization regression coefficient was used to compare the degree to which vegetation and climate affected ET. Thus, the ratio of the absolute values of specific variables to the sum of the absolute values of all variables was the contribution proportion of this variable. Excel 2010 and SPSS 22 were used for the statistical analyses. All of the figures were drawn in Origin 9.2.

Results

Results of model validation

Fig 2 shows that the estimated ET was consistent with the value observed by the E601 evaporator. Monthly evaporation had an RMSD of 14.24 mm and a MAPE of 11.28%, whereas seasonal evaporation had an RMSD of 32.05 mm and a MAPE of 9.08%. The correlation coefficient between the model-estimated and observed data reached 0.876 and 0.921 at monthly and

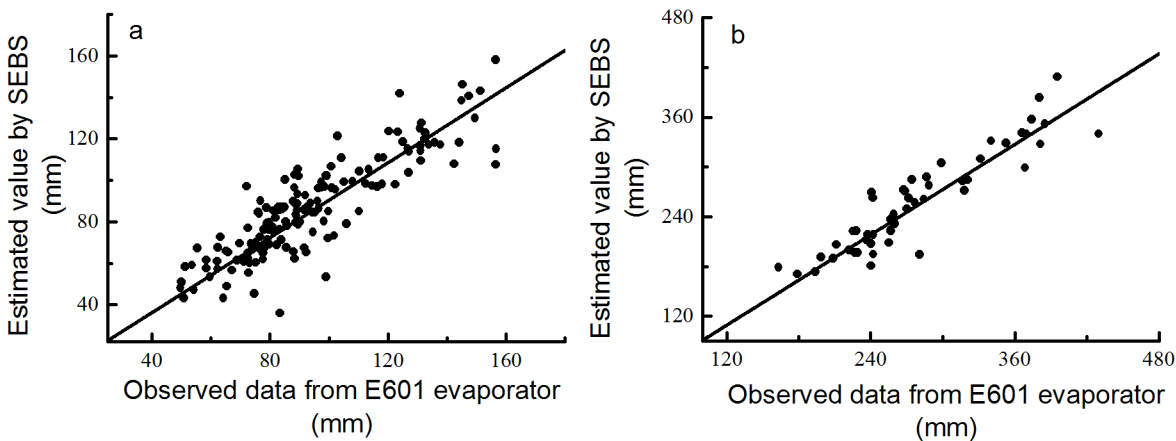


Fig 2. Comparison of water surface evaporation between the SEBS model estimation and observed data from E601. Comparison of water surface evaporation over Erhai Lake between the estimated values and actual observed values at different time scales: (a) monthly water surface evaporation, (b) seasonal water surface evaporation.

doi:10.1371/journal.pone.0134795.g002

seasonal time scales, respectively. Therefore, we concluded that the estimated ET by the SEBS model matched the actual situation in NW Yunnan.

Interannual changes in climatic factors and vegetation coverage

The average annual precipitation and temperature of NW Yunnan varied from 789.41 mm to 1,125.26 mm and from 12.95°C to 14.34°C over the last 13 years, respectively. The linear trend estimation indicated that the temperature significantly increased over time ($P < 0.05$) and the precipitation fluctuated downward but was not statistically significant (Fig 3B). In addition, the average annual relative humidity significantly decreased ($R^2 = 0.683$, $P < 0.01$). Other climatic factors (average wind speed at reference height, total sunshine hours, and downward solar radiation) fluctuated over time without clear trends (Fig 3C and 3D). A correlation analysis revealed that the precipitation was positively correlated with relative humidity and negatively correlated with temperature, sunshine hours, and air pressure, whereas air temperature was negatively correlated with relative humidity at the 0.01 significance level (Table 1). The average annual vegetation coverage was 0.69, ranged from 0.67 to 0.72, and showed a significant increasing trend ($P < 0.01$) over time. However, the NDVI fluctuated without an overall trend.

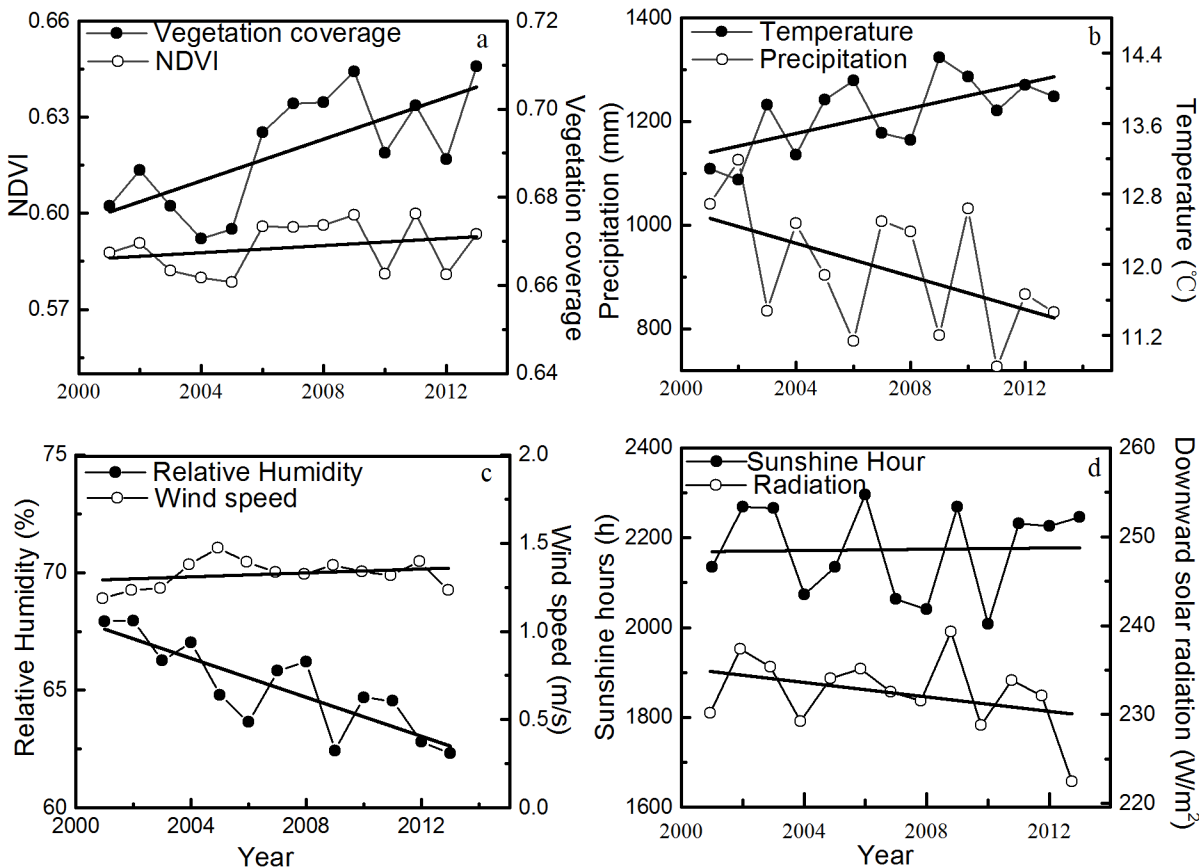


Fig 3. Interannual variations of climate and vegetation coverage. Interannual variations of climate and vegetation coverage: (a) Vegetation coverage and NDVI, (b) temperature and precipitation, (c) relative humidity and wind speed, and (d) sunshine hours and downward solar radiation. Each part of the figure has double Y axes. Each black line represents the linear fit of each variable as a function of the year. Significance tests show that the P-values of (a) vegetation coverage, (b) temperature, and (c) relative humidity were 0.008, 0.017, and 0.000, respectively, whereas the P-values of all other variables were greater than 0.05.

doi:10.1371/journal.pone.0134795.g003

Table 1. Pearson correlation coefficient matrix of climate variables.

	Precipitation	T _{air} ^a	RH ^b	V _{wind} ^c	P _{air} ^d	H _{sunshine} ^e	Ra ^f
Precipitation	1						
T _{air}	-0.713**	1					
RH	0.736**	-0.890**	1				
V _{wind}	-0.291	0.508	-0.434	1			
P _{air}	-0.559*	0.660*	-0.574*	0.603*	1		
H _{sunshine}	-0.590*	0.261	-0.361	-0.16	-0.144	1	
Ra	-0.15	0.086	0.102	0.248	-0.136	0.405	1

^aMean annual air temperature

^brelative humidity

^cwind speed at the reference height

^dair pressure

^etotal annual sunshine hours, and

^fdownward solar radiation.

Asterisks indicate significant differences for climate variables

* indicates $P < 0.05$

** indicates $P < 0.01$.

doi:10.1371/journal.pone.0134795.t001

Interannual changes in ET and WY

The average annual ET (739.27 mm) was lower than the precipitation (919.74 mm) in this area during the study period. However, the ET reached 841.30 and 742.35 mm and the precipitation was only 789.41 and 723.41 mm in 2006 and 2011, respectively, which decreased the WY to below 0 (Fig 4B). The mean ET rate (ratio of ET to precipitation (ET/P)) was 0.80, whereas the WY rate (ratio of WY to precipitation (WY/P)) was only 0.20. Both ET and WY presented considerable fluctuations, with ranging from 623.29 mm to 893.8 mm and -51.88 mm to 384.40 mm, respectively. The ET and WY rates ranged from 0.63 to 1.06 and -0.06 to 0.36, respectively.

Seasonal changes in ET and WY

In general, the highest and lowest ET, precipitation, and WY were recorded in summer and winter, respectively. The mean ET values in spring, summer, autumn, and winter were 219.60,

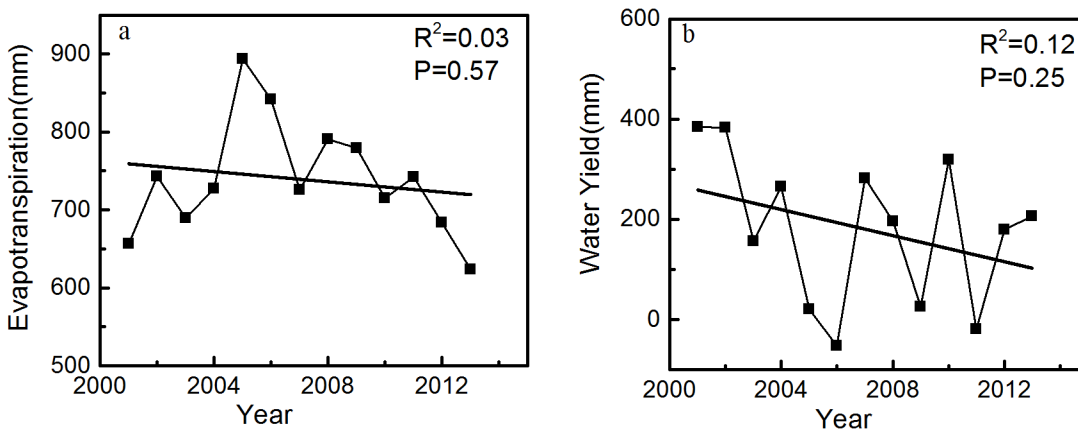


Fig 4. Interannual variations of ET and WY. Interannual variations of ET and WY: (a) ET and (b) WY.

doi:10.1371/journal.pone.0134795.g004

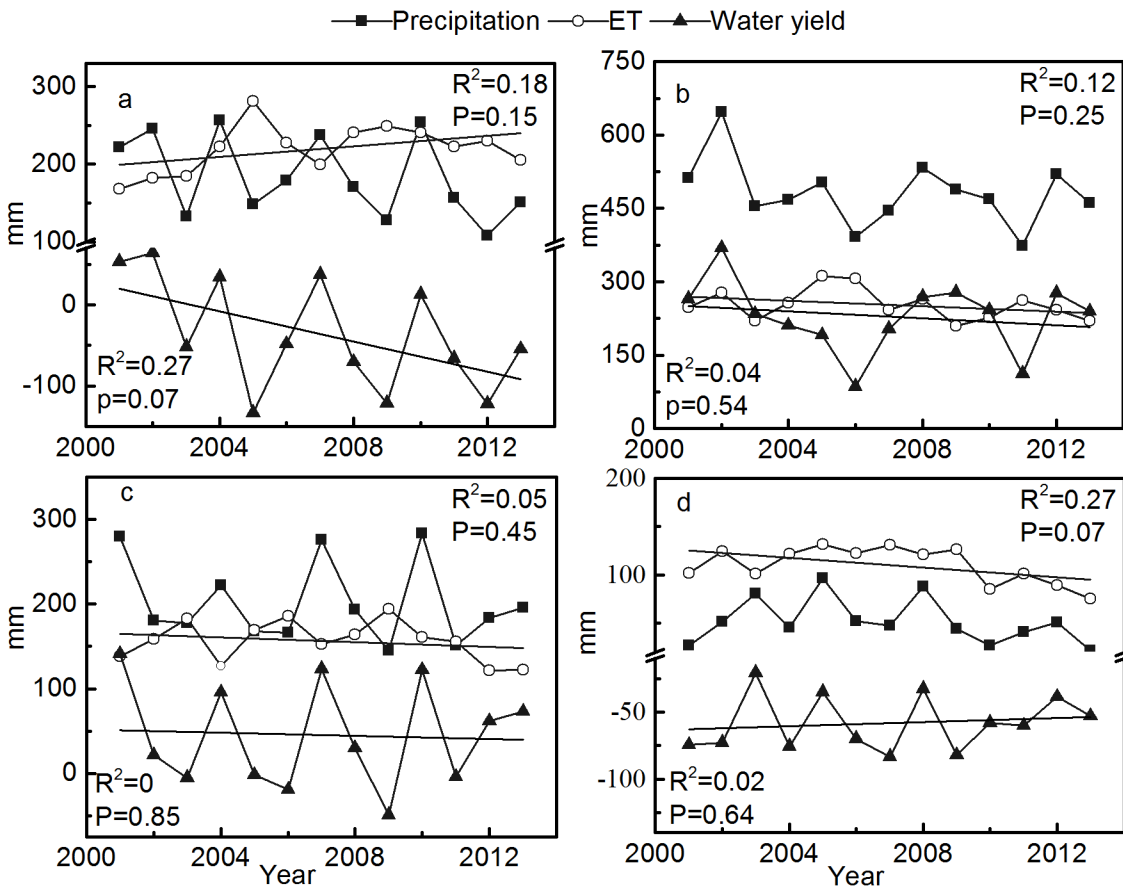


Fig 5. Seasonal changes of ET and WY. Seasonal changes of ET and WY: (a) spring, (b) summer, (c) autumn, and (d) winter. The unit of ET, WY, and precipitation is mm per three months. The trends of seasonal ET and WY are analyzed by linear trend estimation.

doi:10.1371/journal.pone.0134795.g005

252.95, 156.50, and 110.21 mm, respectively. Furthermore, the mean ET values in spring and winter were higher than the precipitation values, resulting in higher ET rates and lower WY rates. The average ET rates in spring, summer, autumn, and winter were 1.30, 0.53, 0.83, and 2.42, respectively, and significant trends were not observed. The WYs of the four seasons also did not show significant trends during the research period, although the WYs in spring decreased more obviously than in any other season because of increasing ET and decreasing precipitation (Fig 5).

Spatial variation of ET and WY

Fig 6 illustrates the variations in ET and WY with time in NW Yunnan. The results of the linear least squares method show that the ET slope exceeded 0 in the southeast area of NW Yunnan, which was primarily in the Dali Bai Autonomous Prefecture and Lijiang City. However, this slope was less than 0 in northwest area of NW Yunnan, which was inaccessible and geographically remote (Fig 6A). Thus, the ET in Dali and Lijiang increased with time, whereas it decreased with time in Diqing and Nujiang. Moreover, F-test showed that ET significantly increased in Lijiang (S1a Fig), where the vegetation coverage also had a significant increase trend (Fig 1). On the other hand, the trend of WY was almost the exact opposite to that of ET (Fig 6B and S1b Fig), which suggests that WY decreased with increasing ET.

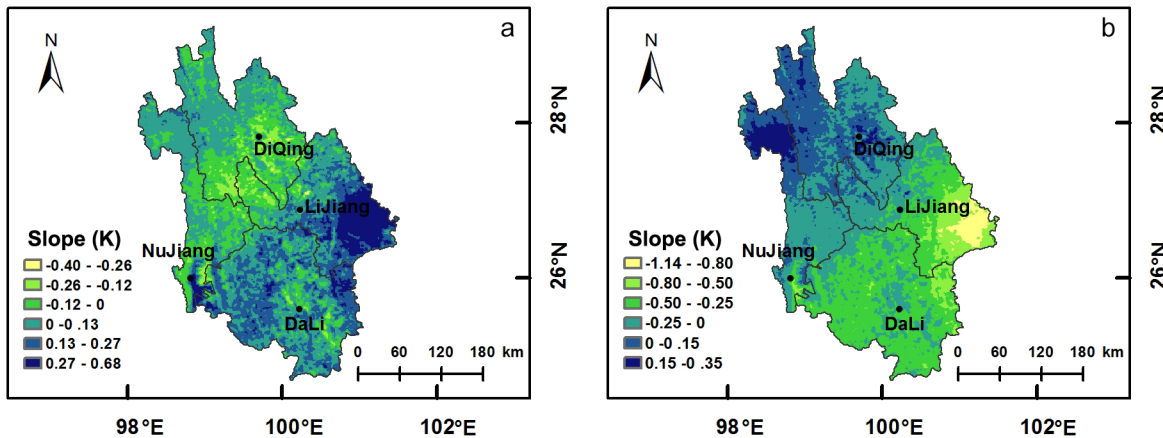


Fig 6. Spatial variations of ET and WY. Maps displaying the slope of ET and WY by linear trend estimation: (a) ET and (b) WY. $K > 0$ and $K < 0$ in any pixels indicate increasing and decreasing trends over time, respectively.

doi:10.1371/journal.pone.0134795.g006

Correlations of ET with climate factors and vegetation coverages

Annual time series data of ET and WY were used for multivariate linear regression analysis. The standardized regression equations are listed in Table 2, and the R^2 values of the regression equations were 0.76, 0.88, 0.90, and 0.88, and each equation reached a significant level (Table 2). The variance inflation factor (VIF) of all variables in the four regression equations was less than 5, which indicated minimal multicollinearity among independent variables. The absolute values of the independent variables in the ET regression equation were ordered as follows: wind speed > relative humidity > vegetation coverage > sunshine hours. Vegetation coverage accounted for 14.82% of the ET (0.426/2.874), and all climatic factors accounted for 85.18% (2.448/2.874) of the ET, which indicated that climatic factors (wind speed, relative humidity, and sunshine hours) were the main cause of ET and vegetation coverage played an integral, although not decisive, role. ET rates, WY, and WY rates were mainly affected by climatic factors, which accounted for 98.92%, 98.88%, and 98.92% of the values, respectively. Precipitation was the main factor that influenced ET rates, WY, and WY rates, and the ratios of precipitation to the total regression coefficient were 53.1%, 67.5%, and 53.1%, respectively. Moreover, precipitation was positively correlated with the WY and WY rate but negatively correlated with

Table 2. Regression analysis of ET and WY.

Dependent variable	Standardized regression equation	R^2	F	P
ET	$Y = 0.856RH^a + 1.199V_{wind}^b + 0.393H_{sunshine}^c + 0.426F_c^d$	0.758	6.272	0.014
ET rate	$Y = -0.686P^e + 0.331V_{wind} + 0.260Ra^f + 0.014F_c$	0.883	15.09	0.001
WY	$Y = 0.782P - 0.362V_{wind} + 0.013F_c$	0.901	27.169	0.000
WY rate	$Y = 0.686P - 0.331V_{wind} - 0.260Ra - 0.014F_c$	0.883	15.09	0.001

^aRelative humidity

^bwind speed at the reference height

^ctotal annual sunshine hours

^dvegetation fraction

^eprecipitation, and

^fdownward solar radiation.

doi:10.1371/journal.pone.0134795.t002

the ET rate. This result indicated that the ET rate increased and WY decreased with decreasing precipitation.

Discussion

Studies have shown that anomalous monsoons induced by ENSO cause weak atmospheric circulation, which results in precipitation deficits in Yunnan [16, 19, 23]. Li et al. (2011) also found that precipitation decreased in the Hengduan Mountains after 2000 [60], which was likely caused by the warm and dry climate [17]. From the perspective of WY, We found that climatic factors (precipitation) greatly influenced the WY (Table 2), and the precipitation deficiency could be considered a main reason for the droughts, which is consistent with the findings of Lü et al. (2012), who studied the physical causes of the severe droughts in the region and drew the same conclusion [18].

In addition, vegetation coverage also explained the changes in WY or ET (Table 2). We found that the contribution of vegetation coverage was small (14.82%) but could not be ignored. Theoretically, climatic factors and human activities are both responsible for vegetation coverage changes, e.g., temperature affects plant phenology or vegetation seasonal dynamics [61, 62], and precipitation positively correlates with vegetation coverage [63, 64]. In NW Yunnan, vegetation coverage markedly increased when precipitation decreased (Table 1), indicating that precipitation was not the major cause of the increased vegetation coverage. We believe that the afforestation/reforestation in recent decades has been the driver of vegetation recovery in Yunnan which has experienced an increase in forest cover from 34% in 1997 to 50% in 2006 with afforestation programs, such as the Natural Forest Protection Program [65]. Plantation forests cover 3.26 million ha, which only account for 17.97% of the total woodland, but the annual growth rate is 17.72% which is greater than that of natural forests (4.08%) [66]. Moreover, Greenpeace indicated that most of the primary forests were replaced by secondary forests (71.18%) and artificial forest (approximately 20%) [32]. Thus, the forest quality deteriorated, despite the cover increasing in recent decades [31, 67]. Studies have shown that the increased ET caused by afforestation/reforestation could reduce WY or runoff [26, 68, 69] and the ET of fast-growing plantation forests was much higher than that of natural primary forests [70–73]. Moreover, in NW Yunnan, remarkable encroachment of woody-plants has been observed in alpine meadows from 1950 to 2009, and at least 39% of the alpine meadows have been converted to woody shrubs [74]. The encroachment of woody plants could also increase the ET of an ecosystem [69].

Spatio-temporal variability of ET and WY matched the actual drought events in Dali and Lijiang in springs (CCTV: <http://english.cntv.cn/program/china24/20120214/110226.shtml>). Dali and Lijiang had a large area of secondary forests of Yunnan pine (*Pinus yunnanensis*), a tree species that is commonly used in afforestation/reforestation [36, 75], whereas the primary natural forests mainly occurred in remote areas, such as Nujiang and Diqing. Differences in the location of primary and secondary growth forests might be one of the reasons for differentiated ET among these prefectures. Although the transpiration data for Yunnan pine forests were unavailable, pine artificial forests have been proven to have higher water consumption than natural forests worldwide [70, 71]. However, Zhang et al. (2011) found that primary and old-growth dark coniferous forests in Southwest China had a lower annual ET and a higher annual WY than shrub lands, regenerated forests, and spruce plantations [76]. Therefore, attention should be paid to ecohydrological effects of human-driven land-cover changes, because higher ET usually implies less water available for human use [77].

Local human populations rely heavily on and are constrained by water resources. Government statistics [40, 78] and water use quota [79] were used in calculations according to Qin

et al. (2014) [80], and we found that the water consumption for primary industry, second industry, tertiary industry and domestic use already accounted for 49.15% of the WY. Primary industry and domestic uses accounted for 75.94% of the total demands and only 9.43% of the total demands was used for industry development. These results indicate that most of the WY was used for subsistence and agricultural production. Because of the poor infrastructure used to extract river water from upstream areas, water provisions from local ecosystems are essential in the mountainous areas of NW Yunnan. Therefore, even a slight ET increase as a result of vegetation changes could significantly increase the system's vulnerability to climate change, especially in rural areas.

Conclusion

Water deficiencies caused by abnormal climate were the primary cause of continuous droughts in NW Yunnan; however, the increased ET resulting from human-driven land-cover and vegetation changes also exacerbated the water shortages. Local human systems are highly vulnerable to climatic drought in term of the water resources provided by its ecosystems. Human disturbances to natural forests as well as massive afforestation/reforestation with several fast-growing tree species are harmful to native biodiversity and increase the system's vulnerability to climate change. In addition to developing infrastructure to mitigate the impacts of droughts, such as irrigation systems and reservoirs, we strongly suggest increasing the conservation efforts related to native vegetation and developing water-conserving agricultural techniques as adaptive strategies to climate change.

Supporting Information

S1 Fig. The trend of ET and WY from 2001 to 2013. The trend of ET and WY: (a) the trend of ET, (b) the trend of WY. F-test is used to test significance of the slopes in Fig 6. The maps are reclassified into different categories according to different significance levels: very significantly ($P < 0.01$), significantly ($P < 0.05$), and slightly ($P > 0.05$). (TIF)

Acknowledgments

We thank the Climatic Data Center, National Meteorological Information Center, China Meteorological Administration for providing meteorological data and NASA for providing the free-downloaded MODIS data.

Author Contributions

Conceived and designed the experiments: HY PL. Performed the experiments: HY JW CM LM ZW YF. Analyzed the data: HY. Contributed reagents/materials/analysis tools: PL HL YY. Wrote the paper: HY PL LDB.

References

1. Gitay H, Suárez A, Watson RT, Dokken DJ. Climate change and biodiversity. Intergovernmental Panel on Climate Change, Geneva, Switzerland; 2002.
2. IPCC. Summary for Policymakers. In: Field CB, Barros VR, Dokken DJ, Mach KJ, Mastrandrea MD, Bilir TE, et al., editors. Climate Change 2014: Impacts, Adaptation, and Vulnerability Part A: Global and Sectoral Aspects Contribution of Working Group II to the Fifth Assessment Report of the Intergovernmental Panel on Climate Change. Cambridge, United Kingdom and New York, NY, USA: Cambridge University Press. 2014.

3. Berrang-Ford L, Ford JD, Paterson J. Are we adapting to climate change? *Global Environ Chang*. 2011; 21: 25–33. doi: [10.1016/j.gloenvcha.2010.09.012](https://doi.org/10.1016/j.gloenvcha.2010.09.012)
4. Chen M, Sun F, Berry P, Tinch R, Ju H, Lin E. Integrated assessment of China's adaptive capacity to climate change with a capital approach. *Climatic Change*. 2014; 128: 367–380. doi: [10.1007/s10584-014-1163-7](https://doi.org/10.1007/s10584-014-1163-7)
5. Yang Y, Tian K, Hao J, Pei S, Yang Y. Biodiversity and biodiversity conservation in Yunnan, China. *Biodivers Conserv*. 2004; 13: 813–826. doi: [10.1023/B:BIOC.0000011728.46362.3c](https://doi.org/10.1023/B:BIOC.0000011728.46362.3c)
6. Cai G, Du M, Liu Y. Regional Drought Monitoring and Analyzing Using MODIS Data—A Case Study in Yunnan Province. In: Li DL, Liu Y and Chen YY, editors. *Computer and Computing Technologies in Agriculture IV*. Berlin, German: Springer Berlin Heidelberg. 2011; pp. 243–251.
7. Qiu J. China drought highlights future climate threats. *Nature*. 2010; 465: 142–143. doi: [10.1038/465142a](https://doi.org/10.1038/465142a) PMID: [20463708](https://pubmed.ncbi.nlm.nih.gov/20463708/)
8. Su Y, Xu J, Wilkes A, Lu J, Li Q, Fu Y, et al. Coping with climate-induced water stresses through time and space in the mountains of Southwest China. *Reg Environ Change*. 2012; 12: 855–866. doi: [10.1007/s10113-012-0304-7](https://doi.org/10.1007/s10113-012-0304-7)
9. Dai A. Drought under global warming: a review. *Wires Clim Change*. 2011; 2: 45–65. doi: [10.1002/wcc.81](https://doi.org/10.1002/wcc.81)
10. Delworth TL, Zeng F. Regional rainfall decline in Australia attributed to anthropogenic greenhouse gases and ozone levels. *Nat Geosci*. 2014; 7: 583–587. doi: [10.1038/ngeo2201](https://doi.org/10.1038/ngeo2201)
11. Cook BI, Miller RL, Seager R. Amplification of the North American "Dust Bowl" drought through human-induced land degradation. *P Natl Acad Sci USA*. 2009; 106: 4997–5001. doi: [10.1073/pnas.0810200106](https://doi.org/10.1073/pnas.0810200106)
12. Fu C. Potential impacts of human-induced land cover change on East Asia monsoon. *Global Planet Change*. 2003; 37: 219–229. doi: [10.1016/s0921-8181\(02\)00207-2](https://doi.org/10.1016/s0921-8181(02)00207-2)
13. Li S, Xiong LH, Dong LH, Zhang J. Effects of the Three Gorges Reservoir on the hydrological droughts at the downstream Yichang station during 2003–2011. *Hydrol Process*. 2013; 27: 3981–3993. doi: [10.1002/hyp.9541](https://doi.org/10.1002/hyp.9541)
14. Zhao C, Deng X, Yuan Y, Yan H, Liang H. Prediction of drought risk based on the wrf model in yunnan province of China. *Adv Meteorol*. 2013; 2013: 9. doi: [10.1155/2013/295856](https://doi.org/10.1155/2013/295856)
15. Lyon B, Christie-Blick N, Gluzberg Y. Water shortages, development, and drought in Rockland County, New York. *J Am Water Resour As*. 2005; 41: 1457–1469. doi: [10.1111/j.1752-1688.2005.tb03812.x](https://doi.org/10.1111/j.1752-1688.2005.tb03812.x)
16. Du H, Yan J. Climate warming-drying and drought-flood tendency judgment of Sichuan-Yunnan region in recent 51 years. *Resources and Environment in the Yangtze Basin*. 2014; 23: 715–721.
17. Li Z. *Spatial and Temporal Variation of Temperature and Precipitation in Southwestern China. Study on Climate Change in Southwestern China*. Berlin, German: Springer Berlin Heidelberg. 2015; pp. 61–100.
18. Lü J, Ju J, Ren J, Gan W. The influence of the Madden-Julian Oscillation activity anomalies on Yunnan's extreme drought of 2009–2010. *Sci China Earth Sci*. 2012; 55: 98–112. doi: [10.1007/s11430-011-4348-1](https://doi.org/10.1007/s11430-011-4348-1)
19. Liu J, Wan J, Tan X, Ma J, Zhang N. Drought in southwest china from autumn 2009 to spring 2010 and its comparative analysis with historical drought events. *Journal of disaster prevention and mitigation engineering*. 2011; 31: 196–200.
20. Yin H, Li Y. Summary of Advance on Drought Study in Southwest China. *J Arid Meteorol*. 2013; 31: 182–193.
21. Huang X, Yu F, Li X, Zheng Y, Yuan H, Ma J, et al. Synthesized attributes of water use by regional vegetation: a key to cognition of "water pump" viewpoint. *The Scientific World Journal*. 2014; 2014: 10. doi: [10.1155/2014/954849](https://doi.org/10.1155/2014/954849)
22. Stone R. Severe Drought Puts Spotlight on Chinese Dams. *Science*. 2010; 327: 1311–1311. doi: [10.1126/science.327.5971.1311](https://doi.org/10.1126/science.327.5971.1311) PMID: [20223955](https://pubmed.ncbi.nlm.nih.gov/20223955/)
23. Zhang W. Did Eucalyptus contribute to environment degradation? Implications from a dispute on causes of severe drought in Yunnan and Guizhou, China. *Environmental Skeptics and Critics*. 2012; 1: 34–38.
24. Belal AA, El-Ramady HR, Mohamed ES, Saleh AM. Drought risk assessment using remote sensing and GIS techniques. *Arab J Geosci*. 2012; 7: 35–53. doi: [10.1007/s12517-012-0707-2](https://doi.org/10.1007/s12517-012-0707-2)
25. Rosenberg NJ, Epstein DJ, Wang D, Vail L, Srinivasan R, Arnold JG. Possible impacts of global warming on the hydrology of the Ogallala aquifer region. *Climatic Change*. 1999; 42: 677–692. doi: [10.1023/a:1005424003553](https://doi.org/10.1023/a:1005424003553)

26. Zhang L, Dawes WR, Walker GR. Response of mean annual evapotranspiration to vegetation changes at catchment scale. *Water Resour Res.* 2001; 37: 701–708. doi: [10.1029/2000wr900325](https://doi.org/10.1029/2000wr900325)
27. Liu M, Tian H. China's land cover and land use change from 1700 to 2005: Estimations from high-resolution satellite data and historical archives. *Global Biogeochem Cy.* 2010; 24: 18. doi: [10.1029/2009gb003687](https://doi.org/10.1029/2009gb003687)
28. Lu Z, Deng X. China's Western Development Strategy: Policies, Effects and Prospects. Munich Personal RePEc Archive. 2011: 1–26.
29. Zhang J, Pham T-T-H, Kalacska M, Turner S. Using Landsat Thematic Mapper records to map land cover change and the impacts of reforestation programmes in the borderlands of southeast Yunnan, China: 1990–2010. *Int J Appl Earth Obs.* 2014; 31: 25–36. doi: [10.1016/j.jag.2014.01.006](https://doi.org/10.1016/j.jag.2014.01.006)
30. Brandt JS, Kuemmerle T, Li H, Ren G, Zhu J, Radeloff VC. Using Landsat imagery to map forest change in southwest China in response to the national logging ban and ecotourism development. *Remote Sens Environ.* 2012; 121: 358–369. doi: [10.1016/j.rse.2012.02.010](https://doi.org/10.1016/j.rse.2012.02.010)
31. Houghton RA, Hackler JL. Sources and sinks of carbon from land-use change in China. *Global Biogeochem Cy.* 2003; 17: 19. doi: [10.1029/2002gb001970](https://doi.org/10.1029/2002gb001970)
32. Wu H, Yi L, Chen S, Liu B. Natural forest in danger—research report of natural forest in Yunnan [Translated from Chinese]. Greenpeace. 2013; 1: 56. Available: <http://www.greenpeace.org/china/Global/china/publications/campaigns/forests/yn-natural-forest-study.pdf>.
33. Melick D, Yang X, Yang Y, Xu J. Establishing long-term biodiversity assessment and monitoring in northwest Yunnan, China: A growing need for baseline information. *Mt Res Dev.* 2006; 26: 292–294. doi: [10.1659/0276-4741\(2006\)26\[292:elbaam\]2.0.co;2](https://doi.org/10.1659/0276-4741(2006)26[292:elbaam]2.0.co;2)
34. Morell V. Letting 1000 forests bloom. *Science.* 2008; 320: 1442–1443. doi: [10.1126/science.320.5882.1442](https://doi.org/10.1126/science.320.5882.1442) PMID: [18556545](https://pubmed.ncbi.nlm.nih.gov/18556545/)
35. Tang Z, Wang Z, Zheng C, Fang J. Biodiversity in China's mountains. *Front Ecol Environ.* 2006; 4: 347–352. doi: [10.1890/1540-9295\(2006\)004\[0347:BICM\]2.0.CO;2](https://doi.org/10.1890/1540-9295(2006)004[0347:BICM]2.0.CO;2)
36. Weyerhaeuser H, Wilkes A, Kahrl F. Local impacts and responses to regional forest conservation and rehabilitation programs in China's northwest Yunnan province. *Agr Syst.* 2005; 85: 234–253. doi: [10.1016/j.agry.2005.06.008](https://doi.org/10.1016/j.agry.2005.06.008)
37. Xu J, Wilkes A. Biodiversity impact analysis in northwest Yunnan, southwest China. *Biodivers Conserv.* 2004; 13: 959–983. doi: [10.1023/b:bioc.0000014464.80847.02](https://doi.org/10.1023/b:bioc.0000014464.80847.02)
38. Yang X, Wilkes A, Yang Y, Xu J, Geslani CS, Yang X, et al. Common and privatized: conditions for wise management of matsutake mushrooms in Northwest Yunnan province, China. *Ecol Soc.* 2009; 14: 30.
39. Yang J. Status and solutions of biodiversity protection in Northwest Yunnan. *For Resour Manag.* 2002; 3: 61–65.
40. Statistic Bureau of Yunnan Province. Yunnan statistical yearbook. Yunnan, China: Statistic Bureau of Yunnan Province; 2001–2013.
41. Liu Y, Zhou Y, Ju W, Chen J, Wang S, He H, et al. Evapotranspiration and water yield over China's land-mass from 2000 to 2010. *Hydrol Earth Syst Sc.* 2013; 17: 4957–4980. doi: [10.5194/hess-17-4957-2013](https://doi.org/10.5194/hess-17-4957-2013)
42. Polasky S, Nelson E, Pennington D, Johnson K. The impact of Land-Use Change on ecosystem services, biodiversity and returns to landowners: A case study in the state of Minnesota. *Environ Resource Econ.* 2011; 48: 219–242. doi: [10.1007/s10640-010-9407-0](https://doi.org/10.1007/s10640-010-9407-0)
43. Sun G, McNulty SG, Lu J, Amatya DM, Liang Y, Kolka RK. Regional annual water yield from forest lands and its response to potential deforestation across the southeastern United States. *J Hydrol.* 2005; 308: 258–268. doi: [10.1016/j.jhydrol.2004.11.021](https://doi.org/10.1016/j.jhydrol.2004.11.021)
44. Su Z, Li X, Zhou Y, Wan L, Wen J, Sintonen K. Estimating areal evaporation from remote sensing. *Geoscience and Remote Sensing Symposium, 2003 IGARSS '03 Proceedings 2003 IEEE International New York.* 2003; 1.2: 1166–1168. doi: [10.1109/IGARSS.2003.1294046](https://doi.org/10.1109/IGARSS.2003.1294046)
45. Su Z. A Surface Energy Balance System (SEBS) for estimation of turbulent heat fluxes from point to continental scale. In: Su Z and Jacobs CMJ, editors. *Advanced Earth Observation, Land Surface Climate.* Netherlands: Publications of the National Remote Sensing Board (BCRS), USP-2. 2001; pp. 91–108.
46. Alkhaier F, Su Z, Flerchinger GN. Reconnoitering the effect of shallow groundwater on land surface temperature and surface energy balance using MODIS and SEBS. *Hydrol Earth Syst Sc.* 2012; 16: 1833–1844. doi: [10.5194/hess-16-1833-2012](https://doi.org/10.5194/hess-16-1833-2012)
47. Chen X, Su Z, Ma Y, Liu S, Yu Q, Xu Z. Development of a 10-year (2001–2010) 0.1° data set of land-surface energy balance for mainland China. *Atmos Chem Phys.* 2014; 14: 13097–13117. doi: [10.5194/acp-14-13097-2014](https://doi.org/10.5194/acp-14-13097-2014)

48. Elhag M, Psilovikos A, Manakos I, Perakis K. Application of the Sebs Water Balance Model in Estimating Daily Evapotranspiration and Evaporative Fraction from Remote Sensing Data Over the Nile Delta. *Water Resour Manag*. 2011; 25: 2731–2742. doi: [10.1007/s11269-011-9835-9](https://doi.org/10.1007/s11269-011-9835-9)
49. Ma W, Ma Y, Hu Z, Su Z, Wang J, Ishikawa H. Estimating surface fluxes over middle and upper streams of the Heihe River Basin with ASTER imagery. *Hydrol Earth Syst Sc*. 2011; 15: 1403–1413. doi: [10.5194/hess-15-1403-2011](https://doi.org/10.5194/hess-15-1403-2011)
50. Su Z. The Surface Energy Balance System (SEBS) for estimation of turbulent heat fluxes. *Hydrol Earth Syst Sc*. 2002; 6: 85–99. doi: [10.5194/hess-6-85-2002](https://doi.org/10.5194/hess-6-85-2002)
51. Allen RG, Pereira LS, Raes D, Smith M. Crop evapotranspiration—Guidelines for computing crop water requirements. FAO Irrigation and drainage paper 1998: 56.
52. Allen RG, Tasumi M, Trezza R. Satellite-based energy balance for mapping evapotranspiration with internalized calibration (METRIC)—Model. *J Irrig Drain E-Asce*. 2007; 133: 380–394. doi: [10.1061/\(asce\)0733-9437\(2007\)133:4\(380\)](https://doi.org/10.1061/(asce)0733-9437(2007)133:4(380))
53. World Meteorological Organization (1976) The CIMO international evaporimeter comparisons. Final Report No 449. Geneva. pp. 6.
54. Fu G, Charles SP, Yu J. A critical overview of pan evaporation trends over the last 50 years. *Climatic Change*. 2009; 97: 193–214. doi: [10.1007/s10584-009-9579-1](https://doi.org/10.1007/s10584-009-9579-1)
55. Wang Y, Huang H. The calculation and features of evaporation in Erhai lake [Translated from Chinese]. *Science and Technology of Dali*. 2007; 2: 9–13.
56. Jing X, Yao W, Wang J, Song X. A study on the relationship between dynamic change of vegetation coverage and precipitation in Beijing's mountainous areas during the last 20 years. *Math Comput Model*. 2011; 54: 1079–1085. doi: [10.1016/j.mcm.2010.11.038](https://doi.org/10.1016/j.mcm.2010.11.038)
57. Liu L, Jing X, Wang J, Zhao C. Analysis of the changes of vegetation coverage of western Beijing mountainous areas using remote sensing and GIS. *Environ Monit Assess*. 2009; 153: 339–349. doi: [10.1007/s10661-008-0360-0](https://doi.org/10.1007/s10661-008-0360-0) PMID: [18516693](https://pubmed.ncbi.nlm.nih.gov/18516693/)
58. Gutman G, Ignatov A. The derivation of the green vegetation fraction from NOAA/AVHRR data for use in numerical weather prediction models. *Int J Remote Sens*. 1998; 19: 1533–1543. doi: [10.1080/014311698215333](https://doi.org/10.1080/014311698215333)
59. Wu B, Li M, Yan C, Zhou W. Developing method of vegetation fraction estimation by remote sensing for soil loss equation: a case in the upper basin of Miyun Reservoir. *IEEE International Geoscience and Remote Sensing Symposium Proceedings, Anchorage, AK*. 2004; 6: 4352–4355. doi: [10.1109/IGARSS.2004.1370101](https://doi.org/10.1109/IGARSS.2004.1370101)
60. Li Z, He Y, Wang C, Wang X, Xin H, Zhang W, et al. Spatial and temporal trends of temperature and precipitation during 1960–2008 at the Hengduan Mountains, China. *Quatern Int*. 2011; 236: 127–142. doi: [10.1016/j.quaint.2010.05.017](https://doi.org/10.1016/j.quaint.2010.05.017)
61. Chen F, Weber KT. Assessing the impact of seasonal precipitation and temperature on vegetation in a grass-dominated rangeland. *Rangeland J*. 2014; 36: 185–190. doi: [10.1071/RJ13098](https://doi.org/10.1071/RJ13098)
62. Yu H, Luedeling E, Xu J. Winter and spring warming result in delayed spring phenology on the Tibetan Plateau. *P Natl Acad Sci USA*. 2010; 107: 22151–22156. doi: [10.1073/pnas.1012490107](https://doi.org/10.1073/pnas.1012490107)
63. Xu X, Yang D, Sivapalan M. Assessing the impact of climate variability on catchment water balance and vegetation cover. *Hydrol Earth Syst Sc*. 2012; 16: 43–58. doi: [10.5194/hess-16-43-2012](https://doi.org/10.5194/hess-16-43-2012)
64. Yang D, Shao W, Yeh PJF, Yang H, Kanae S, Oki T. Impact of vegetation coverage on regional water balance in the nonhumid regions of China. *Water Resour Res*. 2009; 45. doi: [10.1029/2008WR006948](https://doi.org/10.1029/2008WR006948)
65. Frayer J, Sun Z, Müller D, Munroe DK, Xu J. Analyzing the drivers of tree planting in Yunnan, China, with Bayesian networks. *Land Use Policy*. 2014; 36: 248–258. doi: [10.1016/j.landusepol.2013.08.005](https://doi.org/10.1016/j.landusepol.2013.08.005)
66. State Forestry Administration of the People's Republic of China. Seventh National Forest Resource Inventory Report (2004–2008). Beijing, china: State Forestry Administration of the People's Republic of China; 2009.
67. Frayer J, Müller D, Sun Z, Munroe D, Xu J. Processes Underlying 50 Years of Local Forest-Cover Change in Yunnan, China. *Forests*. 2014; 5: 3257–3273. doi: [10.3390/f5123257](https://doi.org/10.3390/f5123257)
68. Brown AE, Zhang L, McMahon TA, Western AW, Vertessy RA. A review of paired catchment studies for determining changes in water yield resulting from alterations in vegetation. *J Hydrol*. 2005; 310: 28–61. doi: [10.1016/j.jhydrol.2004.12.010](https://doi.org/10.1016/j.jhydrol.2004.12.010)
69. Scoot DF, Prinsloo FW, Moses G. A re-analysis of the South African afforestation experimental data. South Africa: Water Research Commission; 2000.
70. Cao G, Wang X, Xiong W, Wang Y, Yu P, Wang Y, et al. Evapotranspiration characteristics of artificial and natural forests in Liupan Mountains of Ningxia, China during growth season. *Chin J Appl Ecol*. 2013; 24: 2089–2096.

71. Licata JA, Gyenge JE, Fernandez ME, Schlichter TA, Bond BJ. Increased water use by ponderosa pine plantations in northwestern Patagonia, Argentina compared with native forest vegetation. *Forest Ecol Manag.* 2008; 255: 753–764. doi: [10.1016/j.foreco.2007.09.061](https://doi.org/10.1016/j.foreco.2007.09.061)
72. Macfarlane C, Bond C, White DA, Grigg AH, Ogden GN, Silberstein R. Transpiration and hydraulic traits of old and regrowth eucalypt forest in southwestern Australia. *Forest Ecol Manag.* 2010; 260: 96–105. doi: [10.1016/j.foreco.2010.04.005](https://doi.org/10.1016/j.foreco.2010.04.005)
73. Tan ZH, Zhang YP, Song QH, Liu WJ, Deng XB, Tang JW, et al. Rubber plantations act as water pumps in tropical China. *Geophys Res Lett.* 2011; 38: L24406. doi: [10.1029/2011gl050006](https://doi.org/10.1029/2011gl050006)
74. Brandt JS, Haynes MA, Kuemmerle T, Waller DM, Radeloff VC. Regime shift on the roof of the world: Alpine meadows converting to shrublands in the southern Himalayas. *Biol Conserv.* 2013; 158: 116–127. doi: [10.1016/j.biocon.2012.07.026](https://doi.org/10.1016/j.biocon.2012.07.026)
75. Wang Z, Lu Y. Compensation for the Conversion of Sloping Farmland to Forest in China: A Feasibility Study of Payment Based on Carbon Sink. *The Journal of Environment & Development.* 2010; 19: 28–41. doi: [10.1177/1070496509338838](https://doi.org/10.1177/1070496509338838)
76. Zhang Y, Liu S, Gu F. The impact of forest vegetation change on water yield in the subalpine region of southwestern China. *Acta Ecol Sin.* 2011; 31: 7601–7609.
77. Weiß M, Schaldach R, Alcamo J, Flörke M. Quantifying the human appropriation of fresh water by African agriculture. *Ecol Soc.* 2009; 14: 25.
78. Water Resources Department of Yunnan Province. Yunnan Province water resource bulletin. Yunnan, China: Water Resources Department of Yunnan Province; 2001–2013.
79. Quality and Technical Supervision Bureau of Yunnan Province. Provincial standard of Yunnan–water quota (DB53/T 186–2013). Yunnan, China: Quality and Technical Supervision Bureau of Yunnan Province; 2013.
80. Qin TL, Yan DH, Wang G, Yin J. Water Demand Forecast in the Baiyangdian Basin with the Extensive and Low-Carbon Economic Modes. *J Appl Math.* 2014; 2014: 1–10. doi: [10.1155/2014/673485](https://doi.org/10.1155/2014/673485)